

Heavy particle dynamics in liquid Se: Inelastic X-ray scattering

Masanori INUI^{1*}, Shinya HOSOKAWA², Kazuhiro MATSUDA³, Satoshi TSUTSUI⁴
and Alfred Q. R. BARON^{4,5}

¹*Graduate School of Integrated Arts and Sciences, Hiroshima University, Higashi-Hiroshima 739-8521*

²*Center for Materials Research using Third-Generation Synchrotron Radiation Facilities, Hiroshima
Institute of Technology, Hiroshima 731-5193*

³*Graduate School of Engineering, Kyoto University, Kyoto 606-8501*

⁴*SPring-8/JASRI 1-1-1 Kouto, Sayo-cho, Sayo-gun, Hyogo-ken 679-5198*

⁵*SPring-8/RIKEN 1-1-1 Kouto, Sayo-cho, Sayo-gun, Hyogo-ken 679-5148*

The dynamic structure factor of liquid Se was measured at 523 K using high-resolution inelastic X-ray scattering. Anomalous narrowing of the spectrum was observed at 15 nm^{-1} , where the static structure factor $S(Q)$ exhibits a weak shoulder, but the elastic part of the dynamic structure factor $S(Q, E = 0)$ exhibited a strong maximum. The second frequency moment, which is estimated from only the quasi-elastic peak, is consistent with the motion of rigid six-atom clusters, while a formal agreement with the first-moment sum rule is preserved by the appearance of a weak intramolecular mode at 30 meV.

KEYWORDS: liquid Se, collective dynamics, inelastic X-ray scattering, de Gennes narrowing

Sum rules for the dynamic structure factor, $S(Q, E)$, where Q and E represent the momentum and energy transfer, respectively, are indispensable for understanding liquid dynamics.¹⁻⁴⁾ For example, the normalized second frequency moment of $S(Q, E)$ expressed as

$$\omega_0^2(Q) = k_B T Q^2 / (m S(Q)), \quad (1)$$

where k_B , T , and m represent the Boltzmann's constant, absolute temperature and particle mass, respectively, predicts that $S(Q, E)$ should be very narrow at the $S(Q)$ maximum in monatomic simple liquids. In fact, narrowing occurs in many simple liquids including liquid metals with a large first maximum in $S(Q)$. This phenomenon is known as de Gennes-narrowing.²⁾

There are other monatomic liquids that exhibit moderate oscillations in $S(Q)$, which means that the first peak is not very large as compared to that in simple liquids. Liquid (l-) Se is one such case. Se forms two-fold coordinated polymeric molecules in both crystalline and liquid states. Crystalline Se, stable at ambient conditions, has a trigonal form wherein three-fold helical chains are hexagonally arranged.⁵⁾ The chain molecule has a bond length of 0.237 nm, a bond angle of 103° , and a dihedral angle of 102° . The valence configuration of

*E-mail address: inui@mls.ias.hiroshima-u.ac.jp

Se is $4s^24p^4$ with two of the 4p electrons in bonding states and the other two forming a lone pair. The exchange repulsion between the adjacent lone pairs in the chain causes these angles to stabilize at approximately 90° .

The regular arrangement of chains in the crystal breaks upon melting; however the chain structure is largely preserved in l-Se as indicated by diffraction measurements.^{6,7)} Other metastable crystalline states are composed of Se_8 ring molecules, including α - and β -monoclinic Se.⁵⁾ The similarity between the medium-range correlation in l-Se and the monoclinic crystals was pointed out⁶⁾ and it is now accepted that in the liquid state, segments with ring-like and helical chain-like configurations are randomly distributed along disordered chains. The average chain length in l-Se was estimated from the viscosity data,⁸⁾ and varied from approximately 10^4 atoms at the melting temperature of 490 K to approximately 800 atoms at 650 K.

Several researchers have studied the coherent dynamics of l-Se using inelastic neutron scattering (INS)⁹⁻¹¹⁾ and a classical molecular dynamics simulation.¹²⁾ The vibrational density of states reported shows maxima at approximately 30 meV and the lower energies corresponding to stretching, bending, and torsional modes in the disordered chain molecules.¹⁰⁾ Now we have measured $S(Q, E)$ of l-Se at 523 K in the Q range from 1.8 to 42.3 nm^{-1} over ± 40 meV, using high-resolution inelastic X-ray scattering (IXS); anomalous narrowing was observed at 15 nm^{-1} where $S(Q)$ does not have a maximum but has a weak shoulder. We will show that the present result is interpreted on the basis of the $\omega_0(Q)$ sum rule by eq. (1).

This experiment has been conducted at the high-resolution IXS beamline (BL35XU) of SPring-8 in Japan.¹³⁾ Backscattering at the Si(11 11 11) reflection was used to provide a beam of 3×10^9 photons/s in a 0.8-meV bandwidth onto the sample. The energy of the incident beam and the Bragg angle of the backscattering were 21.747 keV and 89.98° , respectively. We used ten spherical analyzer crystals at the end of the 10-m horizontal arm. The spectrometer resolution depended on the analyzer crystal and was 1.5-1.8 meV at the present experimental set up. The resolution function was obtained from the measurements of polymethyl methacrylate (PMMA). The momentum transfer resolution ΔQ was 0.6 for Q lower than 5.5 nm^{-1} , and 1.0 nm^{-1} at higher values of Q .

The Se sample of 99.999% purity and 0.04-mm thickness was mounted in a single-crystal sapphire cell,¹⁴⁾ which was contained in a vessel with wide windows made of thin single-crystalline Si. The vessel was filled with 2 bar of He gas of 99.9999% purity in order to reduce evaporation of l-Se. The IXS spectra of l-Se were measured at 523 K. Scans performed over the range from -40 to 40 meV required 3 h, and the total data collection times were 24, 18 and 36 h for the momentum transfers of $Q < 5.5 \text{ nm}^{-1}$, $6.7 < Q < 11 \text{ nm}^{-1}$ and $Q > 11 \text{ nm}^{-1}$, respectively. The backgrounds were measured at 298 K.

We subtracted the background with absorption correction and normalized the spectra by the energy integral of $I(Q, E) - I(Q)$. In order to reveal the overall features of $S(Q, E)$ of

l-Se at 523 K, we plot $I(Q, E)/I(Q) \times S(Q)$ on the E - Q plane in Fig. 1. After normalization of the atomic form factor and polarization factor, the $I(Q)$ value agrees nicely with the value of $S(Q)$ obtained from the static measurements shown in Fig. 2(a). It is noticed that in Fig. 1, the first peak in the elastic part $I(Q, E = 0)/I(Q) \times S(Q)$ is higher than the second one, while the first peak in $S(Q)$ is lower than the second one, as seen in Fig. 2(a). The first peak position in the elastic part shifts to 15 nm^{-1} , which is lower than $Q_1 = 20 \text{ nm}^{-1}$, the first peak position of $S(Q)$. The present result suggests that $S(Q, E)$ is significantly narrow at 15 nm^{-1} . $S(Q, E)$ obtained from INS¹¹) also has a profile similar to the present result.

To evaluate the narrowing at 15 nm^{-1} , we analyzed the data in the framework of generalized hydrodynamics.⁴⁾ Within the generalized Langevin formalism, the classical value of $S(Q, E)/S(Q)$ can be expressed using a complex memory function $M(Q, t)$. Using the real ($\tilde{M}'(Q, E)$) and imaginary ($\tilde{M}''(Q, E)$) parts of the Fourier-Laplace transform of $M(Q, t)$, we obtain the expression⁴⁾

$$\left(\frac{S(Q, E)}{S(Q)} \right)^{ME} = \frac{\pi^{-1} \omega_0^2(Q) \tilde{M}'(Q, E)}{[E^2 - \omega_0^2(Q) + E \tilde{M}''(Q, E)]^2 + [E \tilde{M}'(Q, E)]^2}. \quad (2)$$

We used the viscoelastic model and assumed a memory function with a structural relaxation time $\tau(Q)$ because it provided reasonable fits with χ^2 per degree of freedom of approximately 1, although including a second structural relaxation process would have slightly improved the χ^2 value. Consequently, the total memory function is expressed as

$$M(Q, t) = (\gamma - 1) \omega_0^2(Q) e^{-D_T Q^2 t} + (\omega_\ell^2(Q) - \gamma \omega_0^2(Q)) e^{-t/\tau(Q)}, \quad (3)$$

where $\omega_\ell(Q)$ is the fourth frequency moment and it is related to the sound velocity of an infinite-frequency limit $v_\infty(Q) = \omega_\ell(Q)/Q$. D_T and γ are the thermal diffusivity and specific heat ratio, respectively. They were deduced from the thermodynamic data¹⁵⁻¹⁷⁾ and their Q dependence was neglected. The contribution of the thermal relaxation process to the total memory function was less than 5% in the present analysis. In order to fit the experimental data using this model function, the above expression was modified to satisfy the detailed balance condition and convolved with the resolution function. The parameters $\omega_0(Q)$, $\omega_\ell(Q)$, and $\tau(Q)$ were optimized.

We calculated the longitudinal current-current correlation function $J(Q, E) = (E/Q)^2 S(Q, E)$ using the deconvoluted model function and took the peak position as the energy of the propagating modes $\omega_p(Q)$, which is related to the effective sound velocity $v_p(Q) = \omega_p(Q)/Q$. Figure 2(b) shows $E - Q$ dispersion obtained from the viscoelastic model function. In the low Q region, $\omega_p(Q)$ disperses faster than the adiabatic sound velocity of 1040 m s^{-1} ,¹⁶⁾ following the broken line at approximately 1500 m s^{-1} . $v_\infty(Q)$ deduced from the optimized $\omega_\ell(Q)$ at low Q is approximately 2000 m s^{-1} , while the isothermal sound velocity deduced from $\omega_0(Q)$ was approximately 900 m s^{-1} . As shown in Fig. 2(c), $\tau(Q)$ at the lowest

Q is approximately 2 ps. These results suggest that l-Se lies in the viscoelastic regime even at the lowest Q .

We found the discrepancy between the optimized value of $\omega_0(Q)$ and the value calculated from eq. (1) using $S(Q)$ obtained from a neutron scattering experiment,¹⁸⁾ as shown in Fig. 2(b). The first minimum at 15 nm^{-1} obtained from eq. (1) is shallow. However the optimized $\omega_0(Q)$ value has a deep minimum at 15 nm^{-1} and smaller values than the solid line for $Q > 7 \text{ nm}^{-1}$. How can we understand the present discrepancy in $\omega_0(Q)$? Near the narrowing region around 15 nm^{-1} , our data have excellent statistics and, as shown in Fig. 2(a), the integral of $S(Q, E)$ agrees with $S(Q)$.^{6, 7, 18)} In addition the viscoelastic formula conserves $\omega_0(Q)$ and $\omega_\ell(Q)$.

We have investigated the origin of the apparent discrepancy between the optimized value of $\omega_0(Q)$ and eq. (1). In order to calculate the value of $\omega_0(Q)$ more precisely from the observed $S(Q, E)$, we deconvoluted the IXS spectra using the model function consisting of Gaussian peaks.¹⁹⁾ Here, we do not suggest that the number of Gaussian peaks is equivalent to that of the excitations, but we use the expansion using the error functions to approximate the observed $I(Q, E)/I(Q)$ values. We determined the number of Gaussian peaks in each spectrum on the condition that the value of χ^2 per degrees of freedom is reasonable. Figure 3 shows the best fits of $I(Q, E)/I(Q)$ at 15 nm^{-1} using the viscoelastic and Gaussian model functions. Both models reproduce the quasi-elastic peak at the center, but the viscoelastic model cannot access the small peaks at $\pm 30 \text{ meV}$ corresponding to the stretching mode. We evaluated $\omega_0(Q)$ from the deconvolution using the Gaussian model function and found that it is in better agreement with that denoted by the solid line in Fig. 2(b).

These results imply that when the quasi-elastic peak is broad, the fraction of the small peak at 30 meV to $\omega_0(Q)$ is small, and the viscoelastic and Gaussian models yield similar results. However, when the quasi-elastic peak becomes anomalously narrow, the small peak at 30 meV largely contributes to $\omega_0(Q)$ and the integration removing it yields a much smaller $\omega_0(Q)$ value. These facts suggest a rigid molecule. Previously, the molecular mass of l-N₂ was obtained²⁰⁾ by the application of the first frequency moment sum rule for $S(Q, E)$ that did not include the high-energy region in which the stretching mode existed.²¹⁾ Similarly, for Se, we calculate the Q dependence of m using eq. (1) and estimate the effective mass $m_{eff}(Q)$ from the comparison of the $\omega_0(Q)$ value optimized from the viscoelastic model with the solid curve shown in Fig. 2(b). Figure 4 shows that the $m_{eff}(Q)$, which is denoted by solid circles, is approximately six atoms at 15 nm^{-1} where anomalous narrowing occurs. The large $m_{eff}(Q)$ value is located just around 15 nm^{-1} , while in the other Q region, the $m_{eff}(Q)$ obtained from the viscoelastic model is less than two. Meanwhile, $m_{eff}(Q)$ calculated using $\omega_0(Q)$, including the excitation at 30 meV, shows less anomaly at 15 nm^{-1} .

We consider the physical origin of the large $m_{eff}(Q)$ at 15 nm^{-1} in l-Se obtained from the

viscoelastic model. It is noteworthy that a small shoulder exists in $S(Q)$ at 15 nm^{-1} , as seen in Fig. 2(a). For $S(Q)$ of molecular liquids, the oscillations expressing interatomic correlation are well reproduced using the function $\sin(Qd)/(Qd)$, where d is the interatomic distance.²²⁾ Because the function has the first maximum at $Qd = 2.5\pi$, we estimate $d = 0.52 \text{ nm}$ at 15 nm^{-1} . The covalent bond length of l-Se is approximately 0.235 nm . The second-neighbor distance within a chain is approximately 0.37 nm , and the clear second peak in the radial distribution function in l-Se indicates that the bond angle is maintained at approximately 100° .^{6,7)} Likewise, a valence force field model¹²⁾ suggests that the bond and dihedral angles are distributed around the crystalline values in l-Se to minimize the rotational potentials. The distance of 0.52 nm is approximately equal to the fourth-neighbor distance in both chain and ring molecules. The fourth neighbor is crucial to distinguish between helical-chain and ring-molecule configurations because atoms from the first to the third neighbors are arranged in similar configurations on the same plane in both these molecules. Thus, the position of the fourth neighbor determines the configuration of a segment in the disordered chain: helical chain type or ring type. The $m_{eff}(Q)$ value of approximately six atoms around 15 nm^{-1} suggests that chain- and ring-like segments cooperatively move like a rigid molecule under the propagation of longitudinal waves due to a barrier in the rotational potential. Furthermore, the broad maximum observed in $m_{eff}(Q)$ at around 15 nm^{-1} indicates that the segments at a distance smaller than that of the fourth neighbors contributed to the narrowing, too.

We note that a large effective mass in l-Se was reported by Chiba et al.,¹¹⁾ who analyzed $S(Q, E)$ at high Q ($Q > 70 \text{ nm}^{-1}$) using a free-particle approximation to model their INS spectra. They reported effective masses of 1.7 and 3.5 atoms deduced from the width and recoil energy, respectively. They pointed out that the large effective mass reveals information on the character of the covalent bonds around a struck atom. Although this hints conclusions similar to the results of our experiment, their relatively small effective mass may be attributed to their measurement points at the high Q , corresponding to a smaller length scale.

In conclusion, we measured $S(Q, E)$ of l-Se using high-resolution IXS and found that the quasi-elastic peak becomes anomalously narrow at around 15 nm^{-1} – the location of a small shoulder in $S(Q)$. The sum rule of $\omega_0(Q)$ predicts narrowing at Q_1 in simple liquids.²⁾ We show that anomalous narrowing occurs where $S(Q)$ is not very large, indicating the presence of a rigid cluster with a large effective mass in the polymeric liquid. At large Q values ($Q \rightarrow \infty$), the effective mass should certainly be unity because there is no distinction between free particle motion and the molecular modes. However, at finite Q , the separation of the stretching modes from the quasi-elastic peak in l-Se allowed us to evaluate the particle mass by the application of the second frequency moment sum rule and find peculiar dynamics in the covalent liquid.

The authors would like to thank Prof. K. Tamura, Prof. K. Hoshino, Dr. Y. Katayama, Dr. J. T. Okada, Mr. D. Ishikawa, and Mr. Y. Naito for the valuable discussions. The authors

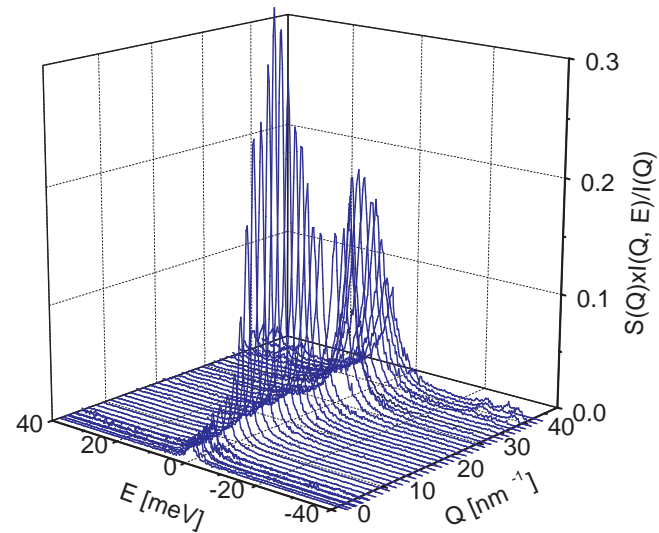


Fig. 1. Overall features of $I(Q, E)/I(Q) \times S(Q)$ of liquid Se at 523 K

thank Prof. K. Maruyama for providing the neutron scattering data. This work is supported by a Grant-in-Aid for Scientific Research from the Ministry of Education, Science and Culture, Japan. The synchrotron radiation experiments were performed at the SPring-8 facility with the approval of the Japan Synchrotron Radiation Research Institute (JASRI) (Proposal No. 2004A0519-ND3d-np).

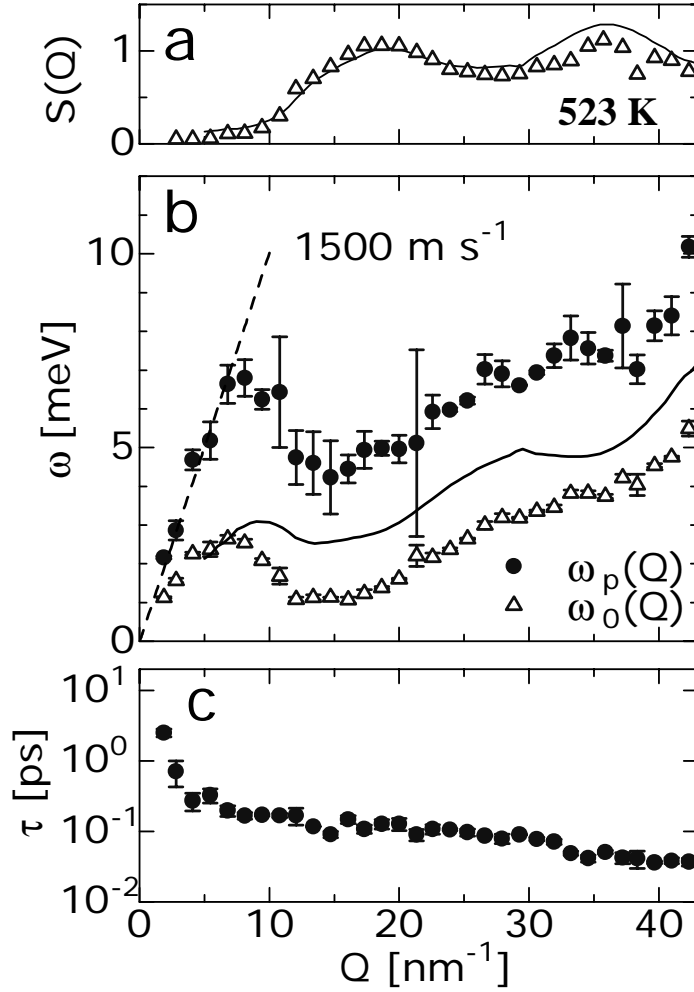


Fig. 2. (a) Static structure factor $S(Q)$ (solid curve) and the integrated intensity of $S(Q, E)$ (open triangles) normalized by the square of the atomic form factor and polarization factor. (b) ω_p (solid circles) and ω_0 (open triangles) at 523 K obtained from the least-squares fits using the viscoelastic model. Also shown are ω_0 deduced from eq. (1) using $S(Q)$ obtained by neutron scattering (solid curve) and dispersion with a slope of 1500 m s^{-1} (broken line). (c) $\tau(Q)$ at 523 K.

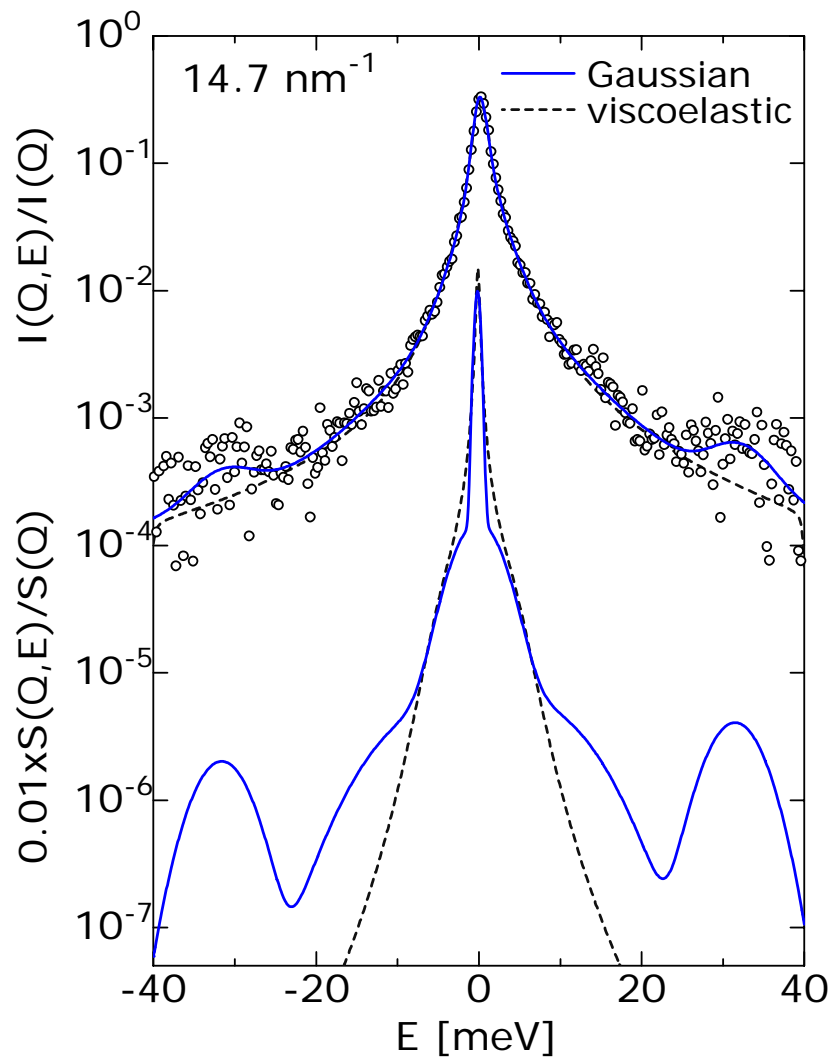


Fig. 3. The best fits of $I(Q, E)/I(Q)$ at 14.7 nm^{-1} and 523 K deduced using the viscoelastic model (broken line) and the Gaussian model (solid line). The open circles denote experimental data. Further, $S(Q, E)/S(Q)$ deconvoluted using both these models are shown at the bottom.

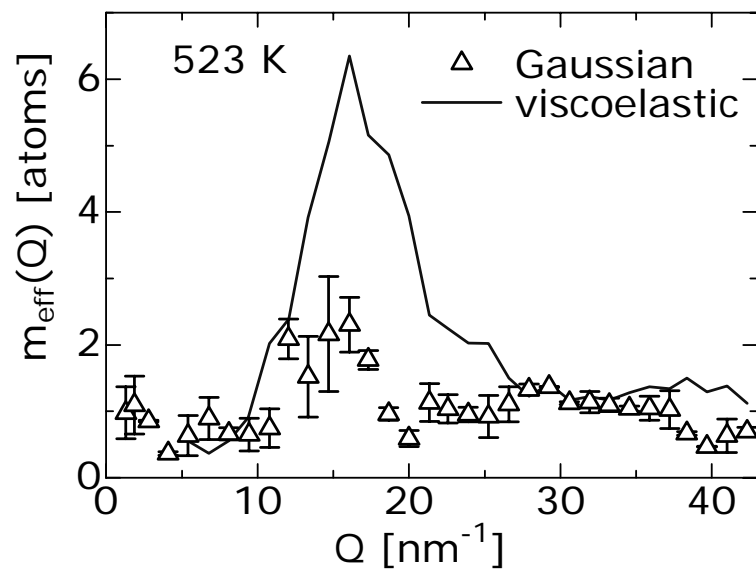


Fig. 4. The effective mass $m_{\text{eff}}(Q)$ at 523 K deduced from the viscoelastic model (solid line) and the Gaussian model (open triangles).

References

- 1) G. Placzek: Phys. Rev. **86** (1952) 377.
- 2) P.G. de Gennes: Physica **25** (1959) 825.
- 3) J. R. D. Copley and S. W. Lovesey: Rep. Prog. Phys. **38** (1975) 461.
- 4) J. P. Boon and S. Yip: *Molecular Hydrodynamics* (McGraw-Hill, New York, 1980) p.35.
- 5) J. Donohue: *The structure of the elements* (John Wiley and Sons, Inc., 1974) p.370.
- 6) Y. Waseda, K. Yokoyama and K. Suzuki: Phys. Cond. Matter **18** (1974) 293.
- 7) M. Misawa and K. Suzuki: Trans JIM **18** (1977) 427.
- 8) A. Eisenberg and A. V. Tobolsky: J. Polym. Sci. **46** (1960) 19.
- 9) A. Axmann, W. Gissler, A. Kollmar and T. Springer, Discuss. Faraday Soc. **50** (1970) 74.
- 10) W. A. Phillips, U. Buchenau, N. Nücker, A.-J. Dianoux and W. Petry: Phys. Rev. Lett. **63** (1989) 2381.
- 11) A. Chiba, Y. Ohmasa and M. Yao: J. Chem. Phys. **119** (2003) 9047.
- 12) N. G. Almarza, E. Enciso and F. J. Bermejo: J. Chem. Phys. **99** (1993) 6876.
- 13) A. Q. R. Baron, Y. Tanaka, S. Goto, K. Takeshita, T. Matsushita and T. Ishikawa: J. Phys. Chem. Solids **61** (2000) 461.
- 14) K. Tamura, M. Inui and S. Hosokawa: Rev. Sci. Instrum. **70** (1999) 144.
- 15) S. Hosokawa, T. Kuboi and K. Tamura: Ber. Bunsenges. Phys. Chem. **101** (1997)120.
- 16) K. Takimoto and H. Endo: Phys. Chem. Liq. **12** (1982) 141.
- 17) L. Ferrari, W. A. Phillips and G. Russo: Europhys. Lett. **3** (1987) 611.
- 18) K. Maruyama, H. Endo and H. Hoshino: J. Phys. Soc. Jpn. **74** (2005) 3213.
- 19) O. Söderström, U. Dahlborg and W. Gudowski: J. Phys. F. **15** (1985) L23.
- 20) K. S. Pedersen, K. Carneiro and F. Y. Hansen: Phys. Rev. A **25** (1982) 3335.
- 21) G. Monaco, M. Nardone, F. Sette and R. Verbeni: Phys. Rev. B **64** (2001) 212102.
- 22) P. A. Egelstaff, D. I. Page and J. G. Powles: Mol. Phys. **20** (1971) 881.